

## Removal of Textile Dyes by Cross Linking Immobilized Bio-Catalyst Enzyme on Quartz Particles: An Experimental Batch and Mathematical Model



Weam Abdulwahhab Mohammed<sup>\*</sup>, Mohanad J. M-Ridha<sup>†</sup>

Environmental Engineering Department, College of Engineering, University of Baghdad, Baghdad 10070, Iraq

Corresponding Author Email: [weam.abd2111p@coeng.uobaghdad.edu.iq](mailto:weam.abd2111p@coeng.uobaghdad.edu.iq)

Copyright: ©2025 The authors. This article is published by IIETA and is licensed under the CC BY 4.0 license (<http://creativecommons.org/licenses/by/4.0/>).

<https://doi.org/10.18280/mmep.120328>

### ABSTRACT

**Received:** 6 January 2024

**Revised:** 22 March 2024

**Accepted:** 30 March 2024

**Available online:** 31 March 2025

#### Keywords:

*biocatalyst enzymes, covalent binding technique, immobilization characteristic, mathematical model, quartz supports*

The aim of this study was to remove the textile dyes Reactive Green 19 (RG19) and Disperse Red 152 (DR152) from the effluent waste by using the immobilized-cabbage legs peroxidase (I-CLP) enzyme. CLP enzyme extractive from restaurant waste was immobilized onto novel support quartz rock (QR) particles with an effective immobilization yield (IY) of  $82 \pm 0.41\%$  through a simple cross-linking covalent technique. The morphological analysis scanning electron microscopy (SEM) and Brunauer-Emmett-Teller (BET) results demonstrate the successful enzyme immobilization. The most prominent experimental conditions used in laboratory work protocols that directly affect the effectiveness and efficiency of the enzyme in removing dyes are pH, temperature, stability, and reuse, which was done in this study. A quantitative model of mass transmission was devised. A great removal for RG19 was observed at 97% and 92% for DR152, representing a high removal of industrial pollutants by enzyme oxidation. The free-cabbage legs peroxidase (F-CLP) and I-CLP enzymes presented their maximum catalytic activities at pH 6 and a temperature of 40°C. After four successive dye decolorization cycles, it can maintain residual activity ranging from 40% to 52%. The immobilization of the biocatalyst enzyme within quartz particles demonstrated significant promise for biotechnological applications, which is considered a cheap, sustainable, and safe method to treat industrial pollutants.

## 1. INTRODUCTION

Due to the scarcity of water and the enormous capacity for wastewater generation brought about by the expansion of industry, research teams are required to focus on developing environmentally friendly products, such as enzymes, as catalysts for treating wastewater [1]. The evaluation and remediation of dye-polluted industrial wastewater effluents are critical processes. Given that certain colors are known to be extremely hazardous to human health, cancer, mutagenic, and the environment, presently used decontamination techniques are either costly or detrimental to human health. Furthermore, many treatment procedures typically result in the buildup of secondary waste products. Green technologies must, therefore, be used to create new techniques for environmental repair [2, 3].

With this context in mind, enzyme-based therapies for removing hazardous dyes provide a far safer alternative to the many physical and chemical approaches currently being employed. A number of benefits, including environmental friendliness, high removal efficiency, specificity, ease of handling, improved standardization, and the capacity to remove a variety of contaminants, have drawn more attention to enzyme-based biological treatments in recent years [4]. It seems to be an environmentally friendly and economically viable choice for decolorization and detoxifying among the

enzymes that could be used for environmental problems. Because of their distinctive characteristics, such as strong activity and selectivity, excellent resistance to substance inhibition across a wide range of concentrations, and reliable performance and durability in various wastewater treatment conditions, dyes and wastewater effluents have garnered a great deal of attention [5], the quick growth period, a minimal amount of land needed for planting, and strong resistance to external factors. As a result, cabbage might provide a different, less costly source of plant enzymes. Plants are a valuable source of the peroxidase catalyst enzyme and can be purchased at reasonable prices from local markets or even repurposed from leftover restaurant waste. Peroxidase (EC 1.11.1.7) is a safe, affordable, and environmentally acceptable catalyst [6]. Free form enzymes are unstable and cannot be repurposed at pH and temperature levels that are not appropriate for medical use, limiting their commercial applicability. Moreover, in organic solvents and during storage, they become unstable [7].

The most efficient method in this situation to overcome these challenges is known to be enzyme immobilization. The immobilized enzyme has a wider range of applications because it produces better separation, increases stability, and can be recycled; covalent bonding is regarded as a dependable method among the recently developed immobilization techniques because soldered supports have several important benefits [8]. The direct covalent linkage between the enzyme

and the nanocomposite can be demonstrated using glutaraldehyde (GA) [9].

These days, the need for sustainable operations has led to a significant increment in the use of enzymes as catalysts in many industrial areas. Additionally, the quick development of protein engineering and extraction/purification techniques has allowed for the effective production of particular enzymes with highly individualized and optimized characteristics at a level of analytical purity [10]. Over the past 20 years, the use of enzymes in a wide range of industrial industries has steadily increased [11]. Figure 1 shows the CBT immobilization technique's industrial and environmental applications. Support materials are essential to the efficiency of an immobilized enzyme because they should be affordable, have a large surface area, and have the least amount of diffusion restriction in the transfer of substrate and product [12, 13].

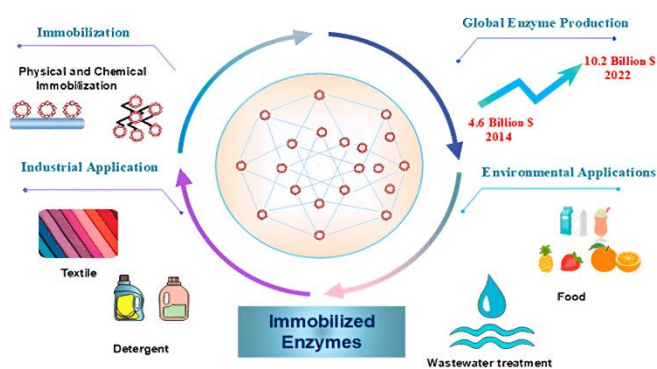


**Figure 1.** Application of immobilization enzyme procedure

The literature discusses a number of immobilization techniques for enzymes, including covalent bonding, ionic adsorption, and van der Waals-based adsorption. The most often reported and utilized method is covalent bonding [14]. Furthermore, a range of supports, including chitosan [15], alginate [16], polyurethane [17], and agar-agar gel [18], can be employed in the immobilization of enzymes.

The purpose of this work was to create a sustainable and environmentally friendly biocatalyst for the decolorization of synthetic dyes by finding a cheap, local source of peroxidase enzyme that is effective in oxidizing pollutants; cabbage legs

might provide a less costly source of plant enzyme. To achieve this, covalent cross-linking between the sold support and CLP was used to immobilize the biocatalyst onto quartz, which was then used to remove RG19 and DR152 from the synthetic solution. The effects of pH, temperature, hydrogen peroxide concentration, protein load, and biocatalyst reuse were among the experimental parameters that were assessed. To calculate the mass transfer coefficients, the kinetic parameters, and the mathematical model. The study found promising results for removing selected industrial dyes by using CLP, with a great removal efficiency for RG19 and DR152.

## 2. MATERIALS AND METHODS

### 2.1 Substances and chemicals

As a peroxidase biocatalyst enzyme, cabbage legs (*Brassica oleracea* var.) CLP were utilized from restaurant waste with specific activity 4977 U/ml, potassium phosphate, sodium acetate, Tris-HCl, H<sub>2</sub>O<sub>2</sub> pyrogallol, 3-amino - propyltriethoxysilane (APTS), were purchased from Sigma-Aldrich, USA, which is classified as the best companies for chemicals used in laboratories. DR152 and RG19 dyes were made in Switzerland and provided by a general textile factory; the chemical construction of textile dyes utilized in the current research is shown in Table 1. QR is inexpensive sold support available in the nature and local market, grind well to obtain 1 mm particles and pass through a sieve mesh 18 stopped at mesh 20, then washed with distilled water and dried in the oven at a temperature of 80°C as illustrated in Figure 2.



**Figure 2.** Particles of QR

**Table 1.** The chemical construction of textile dyes

Dye	$\lambda_{max}$ (nm)	MW (g/mol)	Chemical Structure
DR152	530	452.79	
RG19	545	1418.94	

## 2.2 Methods

### 2.2.1 Extraction of CLP enzyme

In this study, the scientific protocols and techniques used as references were used in extraction, immobilization, preservation, and treatment, as well as chemicals subject to standardization and quality assurance. The biocatalyst Peroxidase was isolated from waste cabbage legs, utilizing a slightly modified version [19].

Wastage cabbage legs weighing 50 g were homogenized for 20 min using 250 ml of phosphate buffer pH 6.5 with 0.2 M. After filtration through two layers of clean cheesecloth in a Cole-Palmer VS-13000 centrifuge, the filtrate was centrifuged at 8000 rpm for 15 minutes. The filter paper was used to filter the carefully collected supernatant into a sterile tube. The material recovered was centrifuged, filtered, and then properly collected and stored as crude enzyme extract CLP at 4°C for subsequent examination.

### 2.2.2 Estimation activity of CLP

Assessment of enzyme activity was measured using pyrogallol as a substrate in the presence of (H<sub>2</sub>O<sub>2</sub>). Purpurogallin, a brownish-orange substance, is created when pyrogallol is oxidized with the assistance of peroxidase. Purpurogallin concentration ( $\lambda$  max = 420 nm,  $\epsilon$  = 4400 M<sup>-1</sup>cm<sup>-1</sup>) was analyzed spectrophotometrically to assess peroxidase activity at room temperature 25°C.

The volume of 3.6 ml reaction mixture contained 1.5 mL of pH 6.5 phosphate buffer, 1.4 mL of 50 mmol L/1 pyrogallol, 0.4 mL of 25 mmol L/1 H<sub>2</sub>O<sub>2</sub>, and 0.3 ml of peroxidase at a concentration of a certain kind. Using a spectrophotometric instrument (UV-9200, BIOTECH ENGINEERING), the difference in absorbance was tracked at 420 nm every minute. In enzyme units per milliliter (U/ml), the enzyme activity was expressed. An enzyme that catalyzes 1.0  $\mu$ mmol of H<sub>2</sub>O<sub>2</sub> per minute at 25°C is considered to have one unit of enzymatic activity (U). Based on Eq. (1), the enzymatic activity was determined. To find the mean value, the analysis was done three times. All experimental conditions and quantities were chosen according to references [20, 21].

$$Activity \left( \frac{U}{mL} \right) = \frac{\left( \frac{dA}{dt} \right) \times AV \times DF}{EV \times \epsilon_{420}} \quad (1)$$

where,  $dA/dt$ : Changing in absorbency per minute. (min<sup>-1</sup>);  $AV$ : Overall volume (3.6 ml);  $DF$ : Dilution factor (1);  $EV$ : Enzyme volume (0.3 ml);  $\epsilon_{420}$ : PurpurOgallin absorptivity at 420 nm (4400 M<sup>-1</sup>cm<sup>-1</sup>).

### 2.2.3 Immobilized enzymes by cross binding techniques

The covalent binding technique (CBT) was used to immobilize the biocatalyst peroxidase with a few minor modifications, and all experimental conditions and quantities were chosen according to reference [22]. A series of functions were used to immobilize the protein at a concentration of 4 mg/ml via covalent linking at 1 g of QR support.

A- 3-aminopropyltriethoxysilane (APTS) 0.5% (v/v) homogenized with quartz particles for at least 4 hours at room temperature using a mechanical shaker.

B- A glutaraldehyde solution with a concentration of 2.5% (v/v) in a volume of 5 mL exposed to the specimen. After eight hours at room temperature, the sample was mechanically stirred.

C- Loading evaluation was used to estimate the amount of

protein needed in the crude enzyme extract. The CBT was utilized. Then, the specimen was kept in static conditions at 4°C for one night.

To get rid of the enzymes that weren't immobilized, the immobilized biocatalysts were washed and filtered. The filtrates were retained throughout the immobilization processes so that peroxidase activity could be measured. The immobilization efficiency of the peroxidase IY%. Eq. (2) represented the peroxidase IY% at quartz particles.

$$IY \% = \frac{\text{Total activity of immobilized CLP}}{\text{Total activity of free CLP}} \times 100\% \quad (2)$$

#### ● The SEM analysis

The SEM technique was used to determine the morphological properties of the supports and the I-CLP by CBT. The solid support samples were analyzed with a scanning electron microscope, and the subsequent SEM images were scrutinized. The microscope was utilized with an accelerating voltage of 15 kilovolts. A layer of 2  $\mu$ m thickness was sputtered onto the samples. Prior to scanning, the initial/immobilized support was dried and coated with nanogold in a vacuum environment to enhance electrical conductivity. SEM was utilized to analyze the surface morphology of the initial, modified, and immobilized particles. Notably, distinct alterations on the particle surface were observed.

#### ● The BET analysis

BET analysis determines the permeability of the structure by examining the adsorption of gas (often nitrogen) on the material's surface. By analyzing the gas (typically nitrogen) that is adsorbed on the surface of the material. The acronym BET, which stands for the names of the scientists who first described this process in the 1930s, can be used to determine the particle diameter, surface area, average pore diameter, and total pore volume.

### 2.2.4 The bio-catalytic characterization of F-CLP and I-CLP

In order to calculate the amount of immobilized enzyme used in dye decolorization, a modified approach is outlined in the pH effect assays: temperature, profile of influence, reuse, and thermal stability [23].

By pre-cultivating the free and immobilized bioenzyme incubation with buffers with variable pH ranging from 4-9, the impact of pH on the relative activities of F-CLP and I-CLP was assessed. By performing a standard activity assay and incubating the free and immobilized enzyme incorporated at different temperatures ranging from 25-80°C, the effect of temperature on the RA for F-CLP and I-CLP was observed. Under typical assay conditions, the thermal stability of the two forms F-CLP and I-CLP were evaluated for 180 minutes at the same condition.

### 2.2.5 Dye decolorization studies

Batch studies utilizing a vessel involving cross linking with CLP previously developed with minor modifications were used to carry out dye decolorization [24]. Every dye (RG19, DR152) solution was put in its beaker. The dye solution was shaken by an 80 rpm rotating stirrer. This stock was utilized to prepare the necessary concentration range of 10-100 mg/l, all of which were done in an aerobic environment. 10 g wet weight of I-CLP was placed in 50 ml Erlenmeyer flasks for the experiments. For eight hours, the flasks were incubated at 45°C.

Then, the dye decolorization was calculated using the relationship given in Eq. (3), with a decrease in optical density acting as a gauge. The complete process mentioned above was repeated numerous times at regular [25].

$$D\% = \frac{A_i - A_f}{A_i} \times 100\% \quad (3)$$

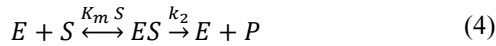
where,  $D\%$ =Decolorization;  $A_i$ =initial absorbance before decolorization;  $A_f$ =final absorbance after incubation.

### 2.2.6 Statistical analysis

The data provided in this study represent the standard deviation ( $\pm$  SD) of triple separate replication studies and are estimated for each treatment and illustrated as error bars in the figures.

### 2.2.7 Kinetic modeling with simulation

The dye decolorization with time in a batch reactor was represented by a mathematical model depending on the kinetic mechanism intended to be used by the equation of Michaelis-Menten. The symbols  $E$ ,  $S$ ,  $ES$ , and  $P$  represent the enzyme, the substrate, the complex combined, and the product, according to the kinetic mechanism proposed by Michaelis-Menten Eq. (4) [26].



where,  $K_{mS}$  and  $k_2$  stand for the rate constant ( $1 \text{ mg}^{-1} \text{ min}^{-1}$ ) and the constant of Michaelis-Menten for substrate ( $\text{mg l}$ ), respectively.

The Michaelis-Menten equation, provided by the following Eq. (5), represents the rate of reaction  $v$  on the concentration of the substrate [26].

$$v = k_2 ES = \frac{v_{max} S}{K_{mS} + S} \quad (5)$$

where, the maximum rate ( $\text{min}^{-1}$ ) and the rate of reaction ( $\text{min}^{-1}$ ) are represented by  $v_{max}$  and  $v$ , respectively. An alternative Michaelis-Menten model can be applied when the removal is incomplete. This model takes into account a reversible Michaelis-Menten mechanism, which is represented by the following Eq. (6).

$$v = \frac{v_{max}(S - \frac{P}{K_{eq}})}{K_{mS}(1 + \frac{P}{K_{mP}}) + S} \quad (6)$$

where,  $K_{eq}$  and  $K_{mP}$  stand for the constant of Michaelis-Menten for the product ( $\text{mg l}^{-1}$ ) and the constant of equilibrium, respectively.

### Batch reactor balance: F-CLP

Eqs. (7) and (8) provide the differential equation that was derived from the mass balance to  $S$  and  $P$  in a batch system while considering the free CLP.

$$-\frac{dS}{dt} = vE \quad (7)$$

$$\frac{dP}{dt} = vE \quad (8)$$

where,  $t$  is time.

### Batch reactor balance: I-CLP

The research [27] served as the inspiration for the mathematical model used to explain elimination in a batch system with immobilized enzymes. The CLP can catalyze a particular reaction in accordance with reversible Michaelis-Menten kinetics; the  $S$  and  $P$  can be simulated by Fick's law model.

Into the catalytic particle through diffusion. Effective diffusivity is concentration-independent and remains constant throughout the particle population. The mass balance for the  $S$  and  $P$  in the liquid bulk phase, respectively, is described by the differential Eqs. (9) and (10) shown below:

$$\frac{dS_b}{dt} = -\frac{(1-\epsilon_r)}{\epsilon_r} \frac{3}{R} k_{LS}(S_b - S_{b,r=R}) \quad (9)$$

$$\frac{dP_b}{dt} = -\frac{(1-\epsilon_r)}{\epsilon_r} \frac{3}{R} k_{LP}(P_b - P_{b,r=R}) \quad (10)$$

where,  $S_b$ ,  $P_b$ ,  $\epsilon_r$ ,  $R$ ,  $k_{LS}$ , and  $k_{LP}$  stand for the concentration of substrate ( $\text{mg l}^{-1}$ ), product ( $\text{mg l}^{-1}$ ), the porosity of particles the radius of particles (m), and mass transfer coefficient by  $S$  and  $P$  ( $\text{m s}^{-1}$ ). In the solid phase for the  $S$  and  $P$  the differential mass balance can be written by the following Eqs. (11) and (12):

$$\epsilon_P \frac{\partial S_P}{\partial t} = \frac{1}{r^2} \frac{\partial}{\partial r} (r^2 D_{eS} \frac{\partial S_P}{\partial r}) - \rho_P v \quad (11)$$

$$\epsilon \frac{\partial P_P}{\partial t} = \frac{1}{r^2} \frac{\partial}{\partial r} (r^2 D_{eP} \frac{\partial P_P}{\partial r}) + \rho_P v \quad (12)$$

where,  $\epsilon_P$ ,  $S_P$ ,  $P_P$ ,  $r$ ,  $D_{eS}$ ,  $D_{eP}$ , and  $\rho_P$  stand for the porosity of particles, substrate concentration in the liquid phase ( $\text{mg l}^{-1}$ ), product concentration in the solid liquid phase ( $\text{mg l}^{-1}$ ), radial coordinate, the effective diffusivity by  $S$  and  $P$  ( $\text{m}^2 \text{ s}^{-1}$ ), and apparent density of the particles ( $\text{kg m}^{-3}$ ), respectively. The boundary conditions for Eqs. (9)-(12) are:

$$t = 0; S_b = S_{b,o}; P_b = S_P = P_P = 0 \quad (13)$$

$$r = 0; \frac{\partial S_P}{\partial r} = \frac{\partial P_P}{\partial r} = 0 \quad (14)$$

where,  $r=R$ .

$$D_{eS} \frac{\partial S_P}{\partial r} = k_{LS}(S_P - S_{P,r=R}) \quad (15)$$

$$D_{eP} \frac{\partial P_P}{\partial r} = k_{LP}(P_P - P_{P,r=R}) \quad (16)$$

where,  $S_{b,o}$  represents the substrate's starting concentration in the bulk phase ( $\text{mg l}^{-1}$ ).

## 3. RESULTS AND DISCUSSION

### 3.1 Cross linking characterization

The SEM morphology of immobilized CLP on quartz particles is displayed in Figure 3. Upon analyzing the photos, it is evident that the immobilization procedure was successful, as evidenced by the considerable amount of enzyme visible on the surface (IY of  $82 \pm 0.41\%$ ). This stands in stark contrast to previous research, which reported a 65% IY for commercial

HRP immobilized on sugarcane bagasse utilizing the CB approach [28]. Using beads with a diameter of 2.0 mm, the reference [29] reported that Ca-alginate encapsulated manganese peroxidase was successfully immobilized with a maximum yield of  $89.3 \pm 2.4\%$  under the most favorable immobilization conditions.

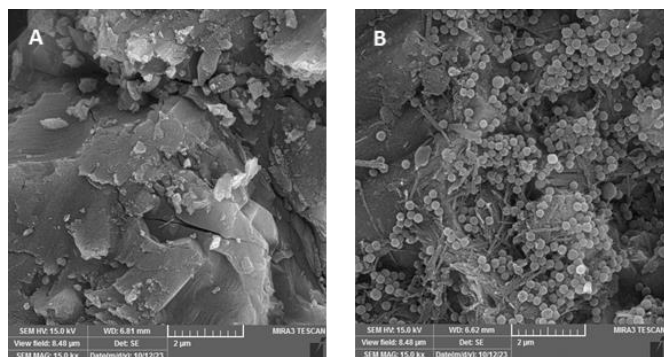


**Figure 3.** SEM image for QR support before and after immobilized enzyme

The BET analysis is a popular tool used to define the chemical and physical properties of porous materials, such as nanomaterials, catalysts, and adsorbents, in a variety of fields, including materials science, bioenvironmental science, and catalysis. This method makes it easier to comprehend how a material performs and to modify its properties for specific uses. At gas pressure of 88 kPa it offers vital details about the pore volume, pore size distribution, and surface area of the material as shown in Table 2 [30].

**Table 2.** The characteristics of immobilized particles by BET analysis

Characteristics	Value
Surface area ( $\text{m}^2/\text{g}$ )	3.38
Overall pore volume ( $\text{cm}^3/\text{g}$ )	0.012
Average pore diameter (nm)	14.246
Particle diameter (mm)	1

### 3.2 The enzyme characterization of F-CLP and I-CLP

#### 3.2.1 Effect of PH on F-CLP and I-CLP

In this experiment, half-unit increments between 4.0 and 9.0 were used to alter the pH of the buffer solutions. The purpose of the study was to compare the reaction rates of immobilized and free CLP preparations at different pH values because the enzyme-substrate interaction can be altered, and the catalytic activity of an enzyme is influenced by pH [31]. To do this, a variety of buffers containing 0.2M sodium acetate buffer for pH ranges 4-5, phosphate buffer ranges 6-7.5, and Tris-HCl buffer ranges 8-9 were utilized. Before measuring the enzyme's activity, both the free and immobilized versions were allowed to incubate for 15 minutes in each of the pertinent buffers. The effect of pH on the relative activity (RA) of F-CLP and I-CLP is shown in Figure 4. It is seen that activity for support increases noticeably at pH 6 with 100% activity, while at pH 5.5 and pH 6.6 it was 92% and 96%, respectively. That will provide a broad range for obtaining high activity of the enzyme, which provides strengths for research. Nonetheless, a decline in activity is noted in basic and acidic environments. This is explained by the way that the CLP and the  $\text{H}^+$  or  $\text{OH}^-$  ions in the buffer interaction, changing

the enzyme microenvironment of the immobilized enzyme, electrostatic interactions with the support might cause alterations in the optimal pH. The enzyme activity decreases seen at elevated pH may have resulted from denaturation [24, 32]. The immobilized gourd peroxidase preparations, as reported in reference [33], exhibited pH optima identical to those of their soluble counterparts, specifically at pH 5.0.

Conversely, other research has shown varying results with gourd peroxidase pH modification, with soluble form values ranging from 5.0 to 4.0 [34].

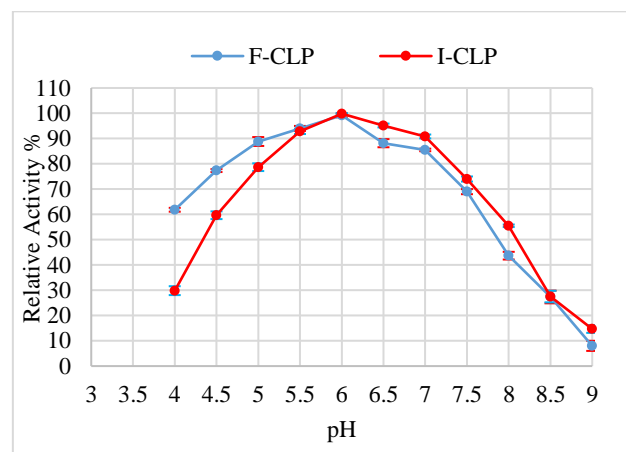


**Figure 4.** Effect of PH on F-CLP and I-CLP relative activity

#### 3.2.2 Effect of temperature on F-CLP and I-CLP

The temperature ranges in which the free and immobilized CLP was evaluated were  $25^\circ\text{C}$  to  $80^\circ\text{C}$ , and each experiment lasted for 15 minutes. The results showed that the peroxidase enzyme maintains its relative activity at  $25\text{--}40^\circ\text{C}$  regardless of whether it is free or immobilized using quartz.

RA was used to express the results. The enzyme thereafter displayed a decline in enzymatic activity. The findings displayed in Figure 5 suggest that  $40^\circ\text{C}$  is the ideal temperature for free peroxidase activity. This discovery is consistent with the outcomes for CLP that have been immobilized. A temperature of  $80^\circ\text{C}$  was shown to retain  $45\% \pm 0.38\%$  of the enzymatic activity of the I-CLP with quartz.

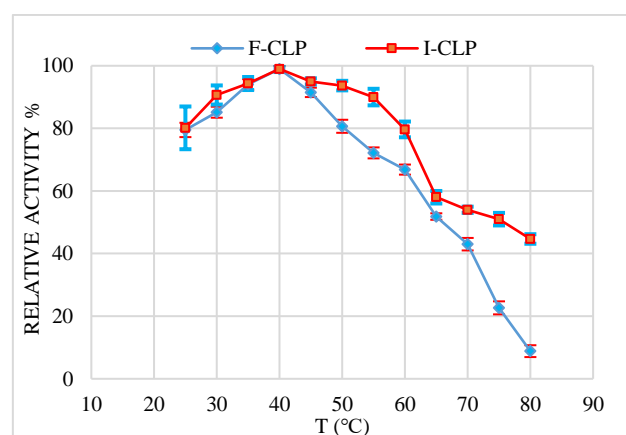


**Figure 5.** Effect of temperature on F-CLP and I-CLP relative activity

It is possible to attribute the observed decrease in free CLP activity with rising temperatures to the protein enzyme's structural modifications, higher mobility, and improved vibrational motion. These changes ultimately cause the

structure of the enzyme to become desaturated and the active site to be disrupted. Evidence that the enzyme is protected from the harmful effects of heat is provided by this behavior [35]. It is plainly useful that this feature ensures the immobilized enzymes can be used at higher operating temperatures, which leads to increased reactivity. According to the report [36], previous research has also observed an increase in temperature following the immobilization of activated wool immobilized HRP.

### 3.2.3 Effect of thermal stability on F-CLP and I-CLP

The temperature of both F-CLP and I-CLP was evaluated by examining their profiles at different temperatures ranging from 25-80°C over 180 min. Enzyme activities were determined over the different time durations of this period [37].

The exhibited responses pertaining to relative activities are illustrated in Figure 6. The results of the study clearly demonstrated that the relative activity of the I-CLP on solid support was significantly greater than that of the F-CLP. The relative activity exhibited a reduction subsequent to pre-incubation at temperatures exceeding 40°C for the free form and 50°C for the immobilized form. The F-CLP was completely inactivated at 80°C while immobilized at quartz and showed residual activity of  $45\% \pm 0.51\%$ ; previous studies have documented an improvement in the thermal resistance of immobilized peroxidases compared to free enzymes. An example of this is the observation that the chitosan beads containing HRP showed a slower decline in activity compared to the enzyme that was not encapsulated. Following a 6-hour incubation at a temperature of 70°C, the free enzyme exhibited a residual activity of 3.2%, whereas the encapsulated enzyme preserved 26.4% of its initial activity [38].

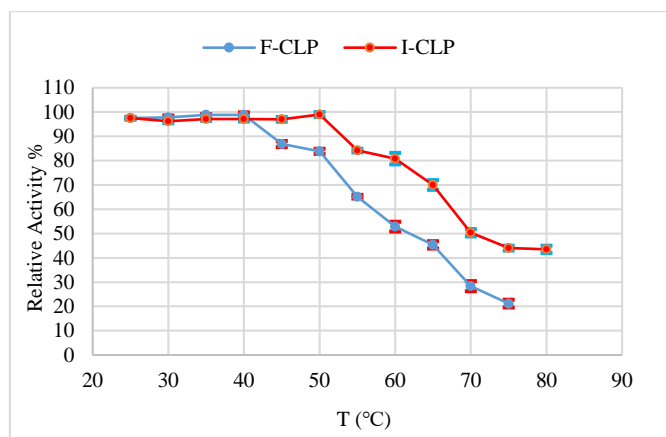


**Figure 6.** Effect of thermal stability on F-CLP and I-CLP relative activity for 180 min

### 3.3 Dyes decolorization by I-CLP

In the batch reactor, the dye-decolorizing potential of I-CLP was examined for two distinct textile dyes: RG19 and DR152. RG had the highest rate of successful dye removal 97% after the I-CLP, followed by DR 92%. The primary goal of immobilization is to ensure that the matrix may be recycled in the batch system. Therefore, the CLP-cross linking with quartz method was used to evaluate the repeatability of I-CLP for the purpose of removing dyes.

Four consecutive catalytic runs were performed in total, and Figure 7 shows the outcomes. Even after four consecutive usages, it was shown that the I-CLP system retained 52-40%

of its operational efficiency. By increasing the number of dye removal runs, the catalytic efficiency of I-CLP was gradually reduced. This could be because the enzyme was leaking from the quartz particle in different amounts or because high-activity free radicals accumulated and entangled the catalytic site of the enzyme, resulting in either product inhibition or enzyme inactivation [39].

>90% of dye-contaminated wastewater degradation was reported in the report [40], which used starch beads to encapsulate peroxidase. When it came to free form, the immobilized peroxidase with polyvinyl alcohol showed better decolorization performance for a number of reactive textile dyes [41].

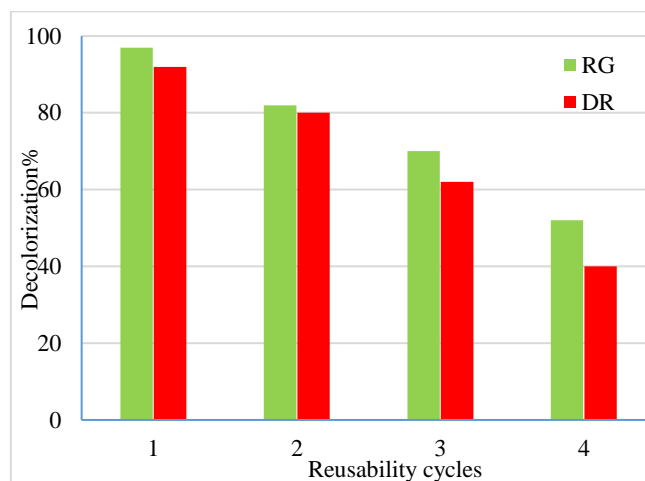


**Figure 7.** Reusability of CLP-immobilized for textile dyes

## 4. CONCLUSIONS

The enzyme CLP was successfully immobilized onto quartz rock particles using a straightforward CBT with an IY of  $82 \pm 0.41\%$ . To obtain the maximum removal efficiency for each textile dye, the characteristics of enzymes, such as temperature, pH, thermal stability, and reusability, have been studied experimentally. On the other hand, immobilized CLP exhibited higher activity than free enzyme, and both dyes were able to employ immobilized enzyme for four cycles in a row. Furthermore, the mass transfer coefficients and kinetic parameters could be found using mass transfer models for both F-CLP and I-CLP. The enzyme immobilized in quartz possesses unique catalytic properties that indicate its suitability for several biotechnological uses, including effluent bioengineering problems.

The research can recommend studying other industrial dyes resulting from textile and dye factories. The immobilized enzyme can also be used to remove other pollutants, such as phenols, heavy metals, and hydrocarbons, which are present in industrial waste thrown into rivers on a large and practical scale.

## REFERENCES

- [1] Arshad, A., Iqbal, J., Mansoor, Q., Ahmed, I. (2017). Graphene/SiO<sub>2</sub> nanocomposites: The enhancement of photocatalytic and biomedical activity of SiO<sub>2</sub> nanoparticles by graphene. *Journal of Applied Physics*, 121(24): 4979968. <https://doi.org/10.1063/1.4979968>

- [2] Calza, P., Zacchigna, D., Laurenti, E. (2016). Degradation of orange dyes and carbamazepine by soybean peroxidase immobilized on silica monoliths and titanium dioxide. *Environmental Science and Pollution Research*, 23: 23742-23749. <https://doi.org/10.1007/s11356-016-7399-1>
- [3] Atiya, M.A., M-Ridha, M.J., Saheb, M.A. (2020). Removal of aniline blue from textile wastewater using electrocoagulation with the application of the response surface approach. *Iraqi Journal of Science*, 2797-2811. <https://doi.org/10.24996/ij.s.2020.61.11.4>
- [4] Bilal, M., Iqbal, H.M., Shah, S.Z.H., Hu, H., Wang, W., Zhang, X. (2016). Horseradish peroxidase-assisted approach to decolorize and detoxify dye pollutants in a packed bed bioreactor. *Journal of Environmental Management*, 183: 836-842. <http://doi.org/10.1016/j.jenvman.2016.09.040>
- [5] Šekuljica, N.Ž., Prlainović, N.Ž., Stefanović, A.B., Žuža, M.G., Čičkarić, D.Z., Mijin, D.Ž., Knežević-Jugović, Z.D. (2015). Decolorization of anthraquinonic dyes from textile effluent using horseradish peroxidase: Optimization and kinetic study. *The Scientific World Journal*, 2015(1): 371625. <https://doi.org/10.1155/2015/371625>
- [6] Chiong, T., Lau, S.Y., Lek, Z.H., Koh, B.Y., Danquah, M.K. (2016). Enzymatic treatment of methyl orange dye in synthetic wastewater by plant-based peroxidase enzymes. *Journal of Environmental Chemical Engineering*, 4: 2500-2509. <https://doi.org/10.1016/j.jece.2016.04.030>
- [7] Krainer, F.W., Glieder, A. (2015). An updated view on horseradish peroxidases: Recombinant production and biotechnological applications. *Applied Microbiology and Biotechnology*, 99: 1611-1625. <https://doi.org/10.1007/s00253-014-6346-7>
- [8] Chang, Q., Tang, H. (2014). Immobilization of horseradish peroxidase on NH<sub>2</sub>-modified magnetic Fe<sub>3</sub>O<sub>4</sub>/SiO<sub>2</sub> particles and its application in removal of 2, 4-dichlorophenol. *Molecules*, 19(10): 15768-15782. <https://doi.org/10.3390/molecules191015768>
- [9] Kandil, O.M., El-Hakim, A.E., Gad, A.A.M., Abu El-Ezz, N.M., Mahmoud, M.S., Hendawy, S.H., Salama, D.B. (2020). Camel hydatidosis diagnostic kit: Optimization of turnip and horseradish peroxidase conjugates using glutaraldehyde method. *Journal of Parasitic Diseases*, 44: 230-238. <https://doi.org/10.1007/s12639-019-01186-4>
- [10] Aziz, G.M., Hussein, S.I., M-Ridha, M.J., Mohammed, S.J., Abed, K.M., Muhamad, M.H., Hasan, H.A. (2023). Activity of laccase enzyme extracted from *Malva parviflora* and its potential for degradation of reactive dyes in aqueous solution. *Biocatalysis and Agricultural Biotechnology*, 50: 102671. <https://doi.org/10.1016/j.bcab.2023.102671>
- [11] Homaei, A. (2015). Enzyme immobilization and its application in the food industry. *Advances in Food Biotechnology*, 145-164. <https://doi.org/10.1002/9781118864463.ch09>
- [12] Zdarta, J., Meyer, A.S., Jesionowski, T., Pinelo, M. (2018). A general overview of support materials for enzyme immobilization: characteristics, properties, practical utility. *Catalysts*, 8(2): 92. <https://doi.org/10.3390/catal8020092>
- [13] Mohamad, N.R., Marzuki, N.H.C., Buang, N.A., Huyop, F., Wahab, R.A. (2015). An overview of technologies for immobilization of enzymes and surface analysis techniques for immobilized enzymes. *Biotechnology & Biotechnological Equipment*, 29(2): 205-220. <https://doi.org/10.1080/13102818.2015.1008192>
- [14] Basso, A., Serban, S. (2019). Industrial applications of immobilized enzymes—A review. *Molecular Catalysis*, 479: 110607. <https://doi.org/10.1016/j.mcat.2019.110607>
- [15] Asgher, M., Noreen, S., Bilal, M. (2017). Enhancing catalytic functionality of *Trametes versicolor* IBL-04 laccase by immobilization on chitosan microspheres. *Chemical Engineering Research and Design*, 119: 1-11. <https://doi.org/10.1016/j.cherd.2016.12.011>
- [16] Ahmedi, A., Abouseoud, M., Abdeltif, A., Annabelle, C. (2015). Effect of diffusion on discoloration of Congo red by alginate entrapped turnip (*Brassica Rapa*) peroxidase. *Enzyme Research*, 2015(1): 575618. <https://doi.org/10.1155/2015/575618>
- [17] Mohy Eldin, M.S., El-Aassar, M.R., El. Zatahry, A.A., Al-Sabah, M.M.B. (2014). Covalent immobilization of  $\beta$ -galactosidase onto amino-functionalized polyvinyl chloride microspheres: enzyme immobilization and characterization. *Advances in Polymer Technology*, 33(1): 21379. <https://doi.org/10.1002/adv.21379>
- [18] Cao, X., Cai, C., Wang, Y., Zheng, X. (2018). The inactivation kinetics of polyphenol oxidase and peroxidase in bayberry juice during thermal and ultrasound treatments. *Innovative Food Science & Emerging Technologies*, 45: 169-178. <https://doi.org/10.1016/j.ifset.2017.09.018>
- [19] Tiwari, B.K. (2015). Ultrasound: A clean, green extraction technology. *TrAC Trends in Analytical Chemistry*, 71: 100-109. <https://doi.org/10.1016/j.trac.2015.04.013>
- [20] Ahmad, Q., Mehmood, A., Saeed, Z., Fayyaz, M. (2019). Purification and characterization of peroxidase from *Brassica oleracea* var. *Acephala*. *Electronic Journal of Biology*, 15(1): 38-45. <https://doi.org/10.1021/jf048162s>
- [21] Aziz, G.M., Hussein, S.I., Abbass, S.D., Ibrahim, A.L., Abbas, D.K. (2021). Degradation of reactive dyes using immobilized peroxidase purified from *Nigella sativa*. *The Iraqi Journal of Agricultural Science*, 52(6): 1365-1374. <https://doi.org/10.36103/ijas.v52i6.1476>
- [22] Queiroz, M.L.B., Conceição, K.C.D., Melo, M.N., Sánchez, O.C., Alvarez, H.M., Soares, C.M., Fricks, A.T. (2018). Immobilization of horseradish peroxidase on sugarcane bagasse. *Química Nova*, 41: 1019-1024. <https://doi.org/10.3390/molecules25163668>
- [23] Silva, M.C., Corrêa, A.D., Amorim, M.T.S.P., Parpot, P., Torres, J.A., Chagas, P.M.B. (2012). Decolorization of the phthalocyanine dye reactive blue 21 by turnip peroxidase and assessment of its oxidation products. *Journal of Molecular Catalysis B: Enzymatic*, 77: 9-14. <https://doi.org/10.1016/j.molcatb.2011.12.006>
- [24] Abou-El-Souod, G., Hamouda, R.A., El-Sheekh, M. (2020). Influence of heavy metal as co-contamination on biodegradation of dyes by free and immobilized *Scenedesmus obliquus*. *Desalination Water Treat*, 182: 351-358. <https://doi.org/10.5004/dwt.2020.25144>
- [25] Alhares, H.S., Shaban, M.A.A., Salman, M.S., M-Ridha, M.J., Mohammed, S.J., Abed, K.M., Ibrahim, M.A., Al-Banaa, A.K., Hasan, H.A. (2023). Sunflower husks coated with copper oxide nanoparticles for reactive blue 49 and reactive red 195 removals: Adsorption

- mechanisms, thermodynamic, kinetic, and isotherm studies. *Water, Air, & Soil Pollution*, 234(1): 35. <https://doi.org/10.1007/s11270-022-06033-6>
- [26] Cristóvão, R.O., Tavares, A.P.M., Ribeiro, A.S., Loureiro, J.M., Boaventura, R.A.R., Macedo, E.A. (2008). Kinetic modelling and simulation of catalyzed degradation of reactive textile dyes. *Bioresource Technology*, 99: 4768-4774. <https://doi.org/10.1016/j.biortech.2007.09.059>
- [27] Al-Muftah, A.E., Abu-Reesh, I.M. (2005). Effects of simultaneous internal and external mass transfer and product inhibition on immobilized enzyme-catalyzed reactor. *Biochemical Engineering Journal*, 27: 167-178. <https://doi.org/10.1016/j.bej.2005.08.026>
- [28] Šekuljica, N.Ž., Prlainović, N.Ž., Lukić, N.M., Jakovljević, A.M., Grbavčić, S.Ž., Mijin, D.Ž., Knežević-Jugović, Z.D. (2015). Immobilization of peroxidase from fresh horseradish extract for anthraquinone dye decolorization. *Zaštita Materijala*, 56(3): 335-339. <https://doi.org/10.5937/savteh1602018S>
- [29] Akhtar, S., Khan, A.A., Husain, Q. (2005). Potential of immobilized bitter gourd (*Momordica charantia*) peroxidases in the decolorization and removal of textile dyes from polluted wastewater and dyeing effluent. *Chemosphere*, 60(3): 291-301. <https://doi.org/10.1016/j.chemosphere.2004.12.017>
- [30] Ali, Q.A., Shaban, M.A.A., Mohammed, S.J., Abd-almohi, H.H., Abed, K.M., Salleh, M.Z.M., Hasan, H.A. (2023). Date palm fibre waste exploitation for the adsorption of Congo red dye via batch and continuous modes. *Journal of Ecological Engineering*, 24(10): 169176. <https://doi.org/10.12911/22998993/169176>
- [31] Mohammadi, M., Heshmati, M.K., Sarabandi, K., Fathi, M., Lim, L.T., Hamishehkar, H. (2019). Activated alginate-montmorillonite beads as an efficient carrier for pectinase immobilization. *International Journal of Biological Macromolecules*, 137: 253-260. <https://doi.org/10.1016/j.ijbiomac.2019.06.236>
- [32] Ladolea, M.R., Pokable, P.B., Patila, S.S., Belokarc, P.G., Pandita, A.B. (2020). Immobilized peroxidase mimicking magnetic metal organic frameworks for industrial dye degradation. *Bioresource Technology*, 317: 124035. <https://doi.org/10.1016/j.biortech.2020.124035>
- [33] Satar, R., Husain, Q. (2011). Catalyzed degradation of disperse dyes by calcium alginate-pectin entrapped bitter gourd (*Momordica Charantia*) peroxidase. *Journal of Environmental Sciences*, 23(7): 1135-1142. [https://doi.org/10.1016/S1001-0742\(10\)60525-6](https://doi.org/10.1016/S1001-0742(10)60525-6)
- [34] Akhtar, S., Khan, A.A., Husain, Q. (2005). Potential of immobilized bitter gourd (*Momordica Charantia*) peroxidases in the decolorization and removal of textile dyes from polluted wastewater and dyeing effluent. *Chemosphere*, 60(3): 291-301. <https://doi.org/10.1016/j.chemosphere.2004.12.017>
- [35] Xie, X., Luo, P., Han, J., Chen, T., Wang, Y., Cai, Y., Liu, Q. (2019). Horseradish peroxidase immobilized on the magnetic composite microspheres for high catalytic ability and operational stability. *Enzyme and Microbial Technology*, 122: 26-35. <https://doi.org/10.1016/j.enzmictec.2018.12.007>
- [36] Diao, M., Dibala, C.I., Ayékoué, B.N.C., Dicko, M.H. (2018). Biochemical characterization of Burkina red radish (*Raphanus Sativus*) peroxidase. *Journal of Applied Biosciences*, 125: 12518-12530. <https://doi.org/10.4314/jab.v125i1.2>
- [37] Vishwasrao, C., Ananthanarayan, L. (2018). Kinetics of inactivation of quality-deteriorating enzymes and degradation of selective phytoconstituents in pink guava pulp during thermal processing. *Journal of Food Science and Technology*, 55: 3273-3280. <https://doi.org/10.1007/s13197-018-3262-3>
- [38] Altinkaynak, C., Tavlasoglu, S., Ocoy, I. (2016). A new generation approach in enzyme immobilization: Organic-inorganic hybrid nanoflowers with enhanced catalytic activity and stability. *Enzyme and Microbial Technology*, 93: 105-112. <https://doi.org/10.1016/j.enzmictec.2016.06.011>
- [39] Zille, A., Tzanov, T., Gübitz, G.M., Cavaco-Paulo, A. (2003). Immobilized laccase for decolourization of Reactive Black 5 dyeing effluent. *Biotechnology Letters*, 25: 1473-1477. <https://doi.org/10.1023/A:1025032323517>
- [40] Ambatkar, M., Mukundan, U. (2015). Enzymatic decolourisation of methyl orange and Bismarck brown using crude peroxidase from *Armoracia rusticana*. *Applied Water Science*, 5: 397-406. <https://doi.org/10.1007/s13201-014-0197-3>
- [41] Husain, Q. (2010). Peroxidase mediated decolorization and remediation of wastewater containing industrial dyes: A review. *Reviews in Environmental Science and Bio/Technology*, 9: 117-140. <https://doi.org/10.1007/s11157-009-9184-9>